DOI: 10.24996/ijs.2022.63.12.26

ISSN: 0067-2904

Hall and Joule Heating Impacts on the Rabinowitsch Fluid in a tapered Channel with Permeable Walls

Rabiha S. Kareem[1], Ahmed M. Abdulhadi[2]

[1]*University of Information Technology and Communications, Baghdad, Iraq*

[2]*Department of Mathematics, College of Science, Baghdad University, Baghdad, Iraq*

Received: 15/8/2021 Accepted: 9/12/2021 Published: 30/12/2022

Abstract

A mathematical model was created to study the influences of Hall current and Joule heating with wall slip conditions on peristaltic motion of Rabinowitsch fluid model through a tapered symmetric channel with Permeable Walls. The governing equations are simplified under low Reynolds number and the long-wavelength approximations. The perturbation method is used to solve the momentum equation. The physiological phenomena are studied for a certain set of pertinent parameters. The effects offered here show that the presence of the hall parameter, coefficient of pseudo-plasticity, and Hartman number impact the flow of the fluid model. Additional, study reveals that a height in the Hall parameter and the velocity slip parameter increases the trapping bolus's apparition. Furthermore, the magnitude of the trapped bolus can be reduced by enhancing the magnetic field.

Keywords: Hall current, Joule heating, Permeable Walls, non-Newtonian fluid, slip conditions, Peristalsis.

تأثيرات تسخين هول وجول على سائل رابينوفيتش في قناة مدببة ذات جدران قابلة للاختراق

رابحة سليم كريم [1]*, احمد مولود عبد الهادي [2]

[1] جامعة تكنولوجيا المعلومات والاتصالات ، بغداد ، العراق

[2] قسم الرياضيات ، كلية العلوم ، جامعة بغداد ، بغداد ، العراق

الخلاصة

بحثت هذه الدراسة في التأثيرات المجمعة لتيار هول وتسخين الجول مع ظروف انزلاق الجدار على الحركة التمعجية لنموذج سائل رابينوفيتش من خلال قناة متناظرة مدببة ذات جدران قابلة للنفاذ. تم تبسيط المعادلات الحاكمة تحت رقم رينولدز المنخفض وتقريب الطول الموجي الطويل. يتم استخدام طريقة الاضطراب لحل معادلة الزخم. تمت دراسة الظواهر الفسيولوجية المذكورة أعلاه لمجموعة معينة من المعلمات ذات الصلة. تظهر التأثيرات المعروضة هنا أن وجود معلمة القاعة ومعامل اللدونة الزائفة ورقم هارتمان يؤثر على تدفق نموذج المائع. كشفت الدراسة كذلك أن الارتفاع في معلمة القاعة ومعلمة انزلاق السرعة يزيدان من ظهور بلعة المحاصرة. علاوة على ذلك ، يمكن تقليل حجم البلعة المحاصرة عن طريق تعزيز المجال المغناطيسي.

*Email: rabiha_s77@yahoo.com

1. Introduction

The fluid movement due to a contraction wave travelling along flexible walls is called peristaltic motion. Peristalsis is one of the most important phenomena of transport mechanisms in many biological systems. In special, the peristaltic phenomenon is important to include the transfer of urine and food through the urinary tract and digestive system, respectively, the movement of the ovum through the fallopian canal and the flow of blood in the little blood vessels. Moreover, this mechanism is involved in designing many biological instruments such as blood pump machines, heart-lung machines, finger pumps, roller pumps and dialysis machines. Many studies on the peristaltic flow of Newtonian and non-Newtonian fluids under the suppositions of Reynolds number and low long-wavelength have been presented in the literature. Some investigations on this topic have been recorded in [1, 2, 3, 4, 5].

Because of their many applications in science and technology, non-Newtonian fluids are currently an important topic. The Rabinowitsch model, which has proven significant for understanding the rheological behavior of biological fluids, has been used to characterize rheological behavior in non-Newtonian fluids. Since it is cubic stress. It also exhibits the characteristics of shear-thinning like blood, Ketchup, and whipped cream. The importance of the model lies in the three main classifications of the various values for the Pseudo-plastic parameter Υ for $\Upsilon = 0$, it represents a Newtonian fluid, for $\Upsilon < 0$, it represents a shear thickening fluid and for $\Upsilon > 0$, it represents a shear-thinning fluid. The experiential effectiveness of this model was presented by Wada and Hayashi[[6]The Rabinowitsch fluid transfer under the peristaltic mechanism was scouted by Akbar and Nadeem [7]. Sing et al. [8] examined the Rabinowitsch fluid model in an elastic peristaltic tube for homogeneous-heterogeneous reactions. Furthermore, studies in the peristaltic mechanism of the Rabinowitsch fluid type can be collected in Refs. [9, 10, 11].

The magnetic field in peristaltic transport has acquired considerable interest due to its variety of comprehensive applications in problems connected with conductive physiological fluids, biomedical engineering, and industry. Such as cell separation, power generators, and cancer tumor treatment. Several related literary works on magnetohydrodynamic on the peristaltic transport [12, 13, 14, 15]. Moreover, the effect of the Hall current cannot be ignored while the electron-atom collision frequency is small or a high magnetic field is considered to be applied. Recent investigations characterizing the Hall influence can be seen through the studies [16, 17, 18].

The current investigation is assisting in filling this gap, we investigate the impact of Hall current and Joule heating into the peristaltic motion of Rabinowitsch fluid in a tapered symmetric porous channel. The problem was formulated by considering wall slip impacts. The governing equations are simplified by assuming the lubrication approach. To determine the solution to the velocity and stream function, the perturbation method is used. Results are analyzed via graphs. Variations of the said quantities with dissimilar parameters are computed by using MATHEMATICA 11 software.

2. Modeling

Investigate incompressible viscous fluid peristaltic flow in the symmetric tapered porous channel with a width of $2d$. Assumed that is a magnetic field B_0. A sinusoidal wave traveling along the axial direction of the channel with c (constant velocity) induces flow, see illustration (Figure 1). Additionally, the thermal effects of Hall and Joule are taken into account. The representation of peristaltic waves on the walls as:

$$\bar{Z} = \bar{H}\,(\bar{X}, \bar{t}) = d + \bar{l}\bar{X} + \bar{\epsilon}\sin\frac{2\pi}{\lambda}(\bar{X} - c\bar{t}) \quad (1)$$

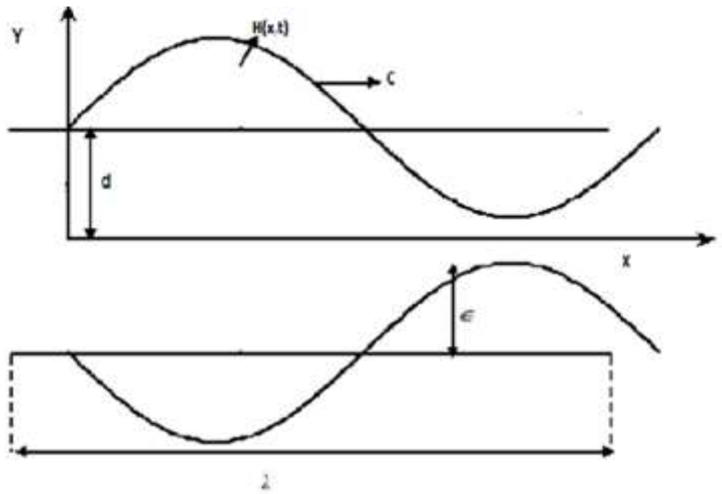

Figure 1: Physical Model

Where $\bar{\epsilon}$ represents the wave amplitude, $\bar{l}(\bar{l} \ll 1)$ represents the non-uniform parameters, $\bar{t}$ represents the time and $\bar{X}$ represents the direction of wave propagation.
The basic equations of the problem for unsteady flow can be written as:

$$\frac{\partial \bar{U}}{\partial \bar{X}} + \frac{\partial \bar{V}}{\partial \bar{Y}} = 0 \tag{2}$$

$$\rho\left(\frac{\partial \bar{U}}{\partial \bar{t}} + \bar{U}\frac{\partial \bar{U}}{\partial \bar{X}} + \bar{V}\frac{\partial \bar{U}}{\partial \bar{Y}}\right) = -\frac{\partial \bar{P}}{\partial \bar{X}} + \frac{\partial \bar{S}_{\bar{X}\bar{X}}}{\partial \bar{X}} + \frac{\partial \bar{S}_{\bar{X}\bar{Y}}}{\partial \bar{Y}} + \frac{\sigma B_0^2}{1+m^2}(-\bar{U} + m\bar{V}) \tag{3}$$

$$\rho\left(\frac{\partial \bar{V}}{\partial \bar{t}} + \bar{U}\frac{\partial \bar{V}}{\partial \bar{X}} + \bar{V}\frac{\partial \bar{V}}{\partial \bar{Y}}\right) = -\frac{\partial \bar{P}}{\partial \bar{Y}} + \frac{\partial \bar{S}_{\bar{Y}\bar{X}}}{\partial \bar{X}} + \frac{\partial \bar{S}_{\bar{Y}\bar{Y}}}{\partial \bar{Y}} - \frac{\sigma B_0^2}{1+m^2}(\bar{V} + m\bar{U}) \tag{4}$$

$$\rho c_p\left(\frac{\partial \bar{T}}{\partial \bar{t}} + \bar{U}\frac{\partial \bar{T}}{\partial \bar{X}} + \bar{V}\frac{\partial \bar{T}}{\partial \bar{Y}}\right) = \kappa\left(\frac{\partial^2 \bar{T}}{\partial \bar{X}^2} + \frac{\partial^2 \bar{T}}{\partial \bar{Y}^2}\right) + (\bar{S}_{\bar{Y}\bar{Y}} - \bar{S}_{\bar{X}\bar{X}})\frac{\partial \bar{U}}{\partial \bar{X}} + \bar{S}_{\bar{X}\bar{Y}}\left(\frac{\partial \bar{U}}{\partial \bar{Y}} + \frac{\partial \bar{V}}{\partial \bar{X}}\right) + \frac{\sigma B_0^2}{1+m^2}(\bar{U}^2 + \bar{V}^2) \tag{5}$$

$$\left(\frac{\partial \bar{C}}{\partial \bar{t}} + \bar{U}\frac{\partial \bar{C}}{\partial \bar{X}} + \bar{V}\frac{\partial \bar{C}}{\partial \bar{Y}}\right) = D_m\left(\frac{\partial^2 \bar{C}}{\partial \bar{X}^2} + \frac{\partial^2 \bar{C}}{\partial \bar{Y}^2}\right) + \frac{D_m K_T}{T_m}\left(\frac{\partial^2 \bar{T}}{\partial \bar{X}^2} + \frac{\partial^2 \bar{T}}{\partial \bar{Y}^2}\right) \tag{6}$$

Where ρ the density of the fluid, $\bar{U}, \bar{V}$ are the axial velocity and transverse velocity, respectively. $\bar{P}, \bar{T}, \bar{C}, B_0, m, \sigma, c_p, \kappa, T_m, K_T$ and D_m denote the pressure, the temperature, the concentration, the magnetic field, the Hall parameter, the electrical conductivity, the specific heat at the constant pressure, thermal conductivity, the mean temperature, the thermal-diffusion ratio and the coefficient of mass diffusivity, respectively.
The extra stress tensor $\bar{S}$ is described by [19] as follows:

$$\bar{S}_{\bar{X}\bar{Y}} + \bar{\Upsilon}\,\bar{S}_{\bar{X}\bar{Y}}^3 = \mu\frac{\partial \bar{U}}{\partial \bar{Y}} \tag{7}$$

In the above equation, $\bar{\Upsilon}$ is the Pseudo-plasticity coefficient and μ is the dynamic viscosity. To normalize the equations governing the flow problem, define the following non-dimensional quantities.

$$x = \frac{\bar{X}}{\lambda},\ y = \frac{\bar{Y}}{d}, t = \frac{c\bar{t}}{\lambda}, \delta = \frac{d}{\lambda}, u = \frac{\bar{U}}{c}, l = \frac{\lambda\bar{l}}{d}, v = \frac{\bar{V}}{\delta c}, \theta = \frac{\bar{T}-T_0}{T_0}, \Upsilon = \frac{c^2\mu^2\bar{\Upsilon}}{d^2}, \phi = \frac{\bar{C}-C_0}{C_0},\ H = \sqrt{\frac{\sigma}{\mu}}dB_0,\ h = \frac{\bar{H}}{d},\ p = \frac{d^2\bar{P}}{c\mu\lambda}, \epsilon = \frac{\bar{\epsilon}}{d}, Sc = \frac{\mu}{\rho\, D_m}, Sr = \frac{\rho D_m K_T(T_0)}{\mu T_m(C_0)},\ Ec = \frac{c^2}{c_p T_0}, Re = \frac{\rho c d}{\mu}, S_{ij} = \frac{d\bar{S}_{ij}}{c\mu},\ P_r = \frac{\mu C_p}{\kappa},\ Br = Ec.Pr \quad (8$$

Where , y are the non-dimensional axial coordinate and transverse coordinate, respectively. t is the non-dimensional time, p is the non-dimensional pressure, δ is the wavenumber, u, v are the non-dimensional axial and transverse velocity components, respectively. The Re is the Reynolds number, S_{ij} is the non-dimensional shear stress, Υ the is non-dimensional coefficient of pseudo-plasticity, θ denotes the non-dimensional temperature, ϕ represents the non-dimensional concentration, Sc is the Schmidt number, H is the Hartman number, h is the non-dimensional transverse wall displacement, Sr is the Soret number, Ec the Eckert number, P_r is the Prandtl and Br is the Birnkman number.

To proceed will employ Eq. (8) in Eqs. (2)-(7),

$$\delta\frac{\partial u}{\partial x}+\frac{\partial v}{\partial y}=0 \tag{9}$$

$$Re\delta\left(\frac{\partial u}{\partial t}+u\frac{\partial u}{\partial x}+v\frac{\partial u}{\partial y}\right)=-\frac{\partial p}{\partial x}+\delta\frac{\partial S_{xx}}{\partial x}+\frac{\partial S_{xy}}{\partial y}+\frac{H^2}{1+m^2}(-u+mv) \tag{10}$$

$$Re\delta^3\left(\frac{\partial v}{\partial t}+u\frac{\partial v}{\partial x}+v\frac{\partial v}{\partial y}\right)=-\frac{\partial p}{\partial y}+\delta^2\frac{\partial S_{yx}}{\partial x}+\delta\frac{\partial S_{yy}}{\partial y}-\frac{H^2\delta}{1+m^2}(v+mu) \tag{11}$$

$$ReP_r\delta\left(\frac{\partial \theta}{\partial t}+u\frac{\partial \theta}{\partial x}+v\frac{\partial \theta}{\partial y}\right)=\delta^2\frac{\partial^2\theta}{\partial x^2}+\frac{\partial^2\theta}{\partial y^2}+Br\delta\left(S_{xx}-S_{yy}\right)\frac{\partial u}{\partial x}+S_{xy}Br\left(\frac{\partial u}{\partial y}+\delta^2\frac{\partial v}{\partial x}\right)+\frac{H^2Br}{1+m^2}(u^2+v^2) \tag{12}$$

$$Re\,S_c\delta\left(\frac{\partial \phi}{\partial t}+u\frac{\partial \phi}{\partial x}+v\frac{\partial \phi}{\partial y}\right)=\delta^2\frac{\partial^2\phi}{\partial x^2}+\frac{\partial^2\phi}{\partial y^2}+SrSc\delta^2\frac{\partial^2\theta}{\partial x^2}+SrSc\frac{\partial^2\theta}{\partial y^2} \tag{13}$$

And

$$(\frac{c\mu}{d})S_{xy}+(\frac{d^2c^3\mu^3}{d^3c^2\mu^2})\Upsilon\,S_{xy}^3=\mu(\frac{c}{d})\frac{\partial u}{\partial y} \tag{14}$$

Defining the stream function by

$$u=\frac{\partial\psi}{\partial y}v=-\delta\frac{\partial\psi}{\partial y} \tag{15}$$

By using the relationship between the velocity and stream function. After some simplification and applying the assumption of low Reynolds number and long wavelength, the problem becomes

$$-\frac{\partial p}{\partial x}+\frac{\partial S_{xy}}{\partial y}-\frac{H^2}{1+m^2}\left(\frac{\partial\psi}{\partial y}\right)=0 \tag{16}$$

$$\frac{\partial p}{\partial y}=0 \tag{17}$$

$$\frac{\partial^2\theta}{\partial y^2}+BrS_{xy}\frac{\partial^2\psi}{\partial y^2}+\frac{H^2Br}{1+m^2}\left(\frac{\partial\psi}{\partial y}\right)^2=0 \tag{18}$$

$$\frac{\partial^2\phi}{\partial y^2}+Sc\,Sr\frac{\partial^2\theta}{\partial y^2}=0 \tag{19}$$

With

$$S_{xy}+\Upsilon\,S_{xy}^3=\frac{\partial^2\psi}{\partial y^2} \tag{20}$$

The non-dimensional boundary conditions are provided by [10].

$$\frac{\partial\psi}{\partial y}=-1-\frac{\sqrt{Da}}{\beta}\frac{\partial^2\psi}{\partial y^2}=0 \quad at \quad y=h \tag{21}$$

$$\theta+\beta_1\frac{\partial\theta}{\partial y}=0 \quad at \quad y=h \tag{22}$$

$$\phi+\alpha_1\frac{\partial\phi}{\partial y}=0 \quad at \quad y=h \tag{23}$$

$$\frac{\partial^2\psi}{\partial y^2}=0,\psi=0,\ \frac{\partial\theta}{\partial y}=0,\ \frac{\partial\phi}{\partial y}=0 \quad at\ y=0 \tag{24}$$

Where Da and β the dimensionless permeability parameter and the slip velocity at the nominal surface respectively. The first boundary condition is following Saffman [20] which is a developed condition to the Beavers and Joseph slip condition. β_1 and α_1 represent the dimensionless thermal and concentration slip parameters. With the dimensionless formula of the channel wall is

$$z = h = 1 + lx + \epsilon \sin 2\pi(x - t) \quad (25)$$

Because the governing boundary value issue can be solved exactly, one can write that using integrating equation (16) and boundary condition (24).

$$S_{xy} = \frac{\partial p}{\partial x} y + \frac{H^2}{1+m^2} \psi \quad (26)$$

Now, employing Eq. (26) in Eq. (20), we obtain the following

$$\frac{\partial p}{\partial x} y + \frac{H^2}{1+m^2} \psi + \Upsilon \left(\frac{\partial p}{\partial x} y + \frac{H^2}{1+m^2} \psi \right)^3 = \frac{\partial^2 \psi}{\partial y^2} \quad (27)$$

Where $\frac{\partial p}{\partial x}$ can be found by using the volumetric flux

$$Q = \int_0^h u(x, y) dy \quad (28)$$

The dimensionless time-averaged flux Q across one wavelength is

$$F = \int_0^1 \int_0^{h(x)} y(u - 1) dx dy = Q + 1 + \frac{\epsilon^2}{2} \quad (29)$$

3. Solution methodology

Eq.(27) is hard to be solved exactly. Thus perturbation technique is applied to find series of solutions for the small parameters. By perturbation, the stream function ψ about Rabinowitsch fluid. Using the following expansion to Υ.

$$\psi = \psi_0 + \Upsilon \psi_1 + O(\Upsilon^2) \quad (30)$$

3.1. *Zeroth-order*

The resulting zeroth-order system has the form

$$\frac{\partial p}{\partial x} y + \frac{H^2}{1+m^2} \psi_0 = \frac{\partial^2 \psi_0}{\partial y^2} \quad (31)$$

Associated with the boundary conditions

$$\frac{\partial \psi_0}{\partial y} = -1 - \frac{\sqrt{Da}}{\beta} \frac{\partial^2 \psi_0}{\partial y^2} = 0 \quad at \quad y = h \quad (32)$$

$$\frac{\partial^2 \psi_0}{\partial y^2} = 0 \quad at\ y = 0 \quad (33)$$

3.2. *First-order*

$$\left(\frac{H^2}{1+m^2}\right) \psi_1 + \left(\frac{\partial p}{\partial x}\right)^3 y^3 + 3\left(\frac{H^2}{1+m^2}\right)\left(\frac{\partial p}{\partial x}\right)^2 y^2 \psi_0 + 3\left(\frac{H^2}{1+m^2}\right)^2 \left(\frac{\partial p}{\partial x}\right) y \psi_0^2 + \left(\frac{H^2}{1+m^2}\right)^3 \psi_0^3 = \frac{\partial^2 \psi_1}{\partial y^2} \quad (34)$$

Associated with the boundary conditions

$$\frac{\partial \psi_1}{\partial y} = -\frac{\sqrt{Da}}{\beta} \frac{\partial^2 \psi_1}{\partial y^2} = 0 \quad at \quad y = h \quad (35)$$

$$\frac{\partial^2 \psi_1}{\partial y^2} = 0 \quad at\ y = 0 \quad (36)$$

By solving the zero and first-order systems using the Mathematica program, the final solution stream function is given as

$$\psi_{0=} - \frac{e^{-\sqrt{n}y} \begin{pmatrix} -\sqrt{Da} e^{\sqrt{n}y} npy + \sqrt{Da} e^{2h\sqrt{n}+\sqrt{n}y} npy - \\ e^{h\sqrt{n}} n\beta + e^{h\sqrt{n}+2\sqrt{n}y} n\beta + e^{h\sqrt{n}} hp\beta - e^{h\sqrt{n}+2\sqrt{n}y} hp\beta - e^{\sqrt{n}y} py\beta + e^{2h\sqrt{n}+\sqrt{n}y} py\beta \end{pmatrix}}{\left(-1 + e^{2h\sqrt{n}}\right) n \left(\sqrt{Da} n + \beta\right)} \quad (37)$$

$$\psi_1 = -\frac{1}{8\left(-1 + e^{h\sqrt{n}}\right)^4 \left(1 + e^{h\sqrt{n}}\right)^4 n\left(\sqrt{Da} n + \beta\right)^4} e^{-\sqrt{n}y} \beta^3 (-9\sqrt{Da} e^{h\sqrt{n}} n^4 + 18\sqrt{Da} e^{3h\sqrt{n}} n^4 - 18\sqrt{Da} e^{5h\sqrt{n}} n^4 + 9\sqrt{Da} e^{7h\sqrt{n}} n^4 - \cdots \quad (38)$$

The temperature and concentration expression are obtained by solving equations (18) and (19) with boundary conditions (22)-(24)

$$\theta = (12 e^{2\sqrt{n}y} y^4 (BrDa e^{6h\sqrt{n}} n^{10} \beta^6 \kappa^2 - 2BrDa e^{8h\sqrt{n}} n^{10} \beta^6 \kappa^2 + BrDa e^{10h\sqrt{n}} n^{10} \beta^6 \kappa^2 - 6BrDa e^{6h\sqrt{n}} h n^9 p \beta^6 \kappa^2 + \ \ldots \quad (39)$$

$$\phi = -((12 e^{4\sqrt{n}y} y^4 (BrDa e^{6h\sqrt{n}} n^{10} ScSr \beta^6 \kappa^2 - 2BrDa e^{8h\sqrt{n}} n^{10} ScSr \beta^6 \kappa^2 + BrDa e^{10h\sqrt{n}} n^{10} ScSr \beta^6 \kappa^2 - 6BrDa e^{6h\sqrt{n}} h n^9 p ScSr \beta^6 \kappa^2 + \cdots \quad (40)$$

Where $n = \frac{H^2}{1+m^2}$

4. Results and discussion

The major purpose of this part is study the impact of various physical parameters on velocity, temperature, concentration, and trapping. Consequently, the graphical outcomes are numerically acquired in Mathematica software. The suitable physical illustrations are shown in this section. Figure 2 is schemed to see the influence of Υ, m, H, and Da on velocity distribution. The dependence of the coefficient of pseudo-plasticity on the axial velocity is shown in Figure 2(a). It is evident from Figure 2(a) effect of the parameter Υ to the sides of the channel, increases the axial velocity in this region, while it decreases in the core region. Figure 2(b) shows the growing influence of velocity distribution for rising Hall parameter m. Actually, with an increased Hall parameter, the effective conductivity declines. So, it reasons a reduction in magnetic force and thus velocity distribution improves. Figure 2(c) describes Hartman number H's effects on the velocity distribution. The attained results show axial velocity reduced in the center channel and raise near the channel walls with the rise in the value of H. Physically, this is because increases Lorentz force reductions the velocity. It is also noticed from Figure 2(d), decreasing behavior of axial velocity with the permeability parameter Da increases.

The response of temperature toward inserted parameters is highlighted in Figure 3. The influence of the Brinkman number Br on temperature distribution is depicted in Figure 3(a). When the Br is increased, it is obvious that the temperature rises. This impact is caused by more viscous dissipation, which generates more heat and hence causes a temperature increase. Axial temperature declines as we grow Hartman number H (see Figure 3(b)). As seen in Figure 3(c), raising the value of the thermal slip parameter β_1 reduces the temperature distribution. In Figure 3(d), the Hall parameter m exhibits the reverse behavior. When m is increased, there is a minor increase in the maximum temperature value. The result demonstrates that m resists the fluid change caused by an increase in the applied magnetic field strength.

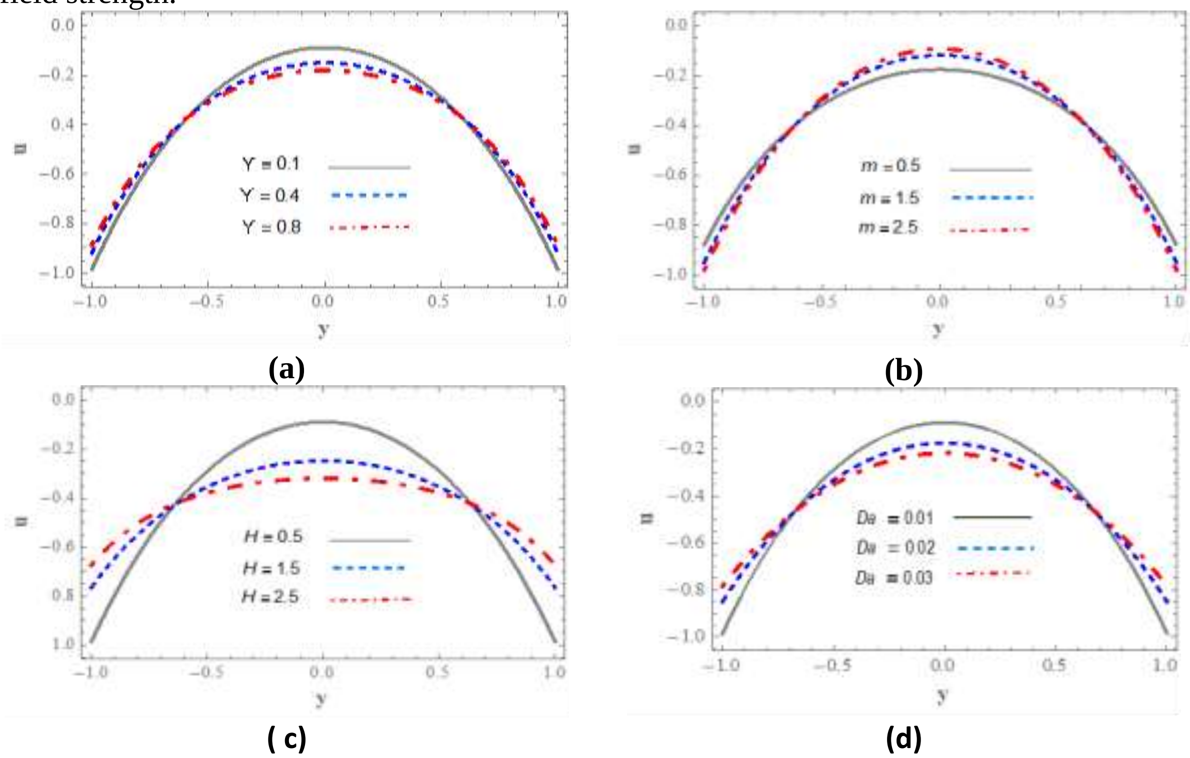

Figure -2 Influence of **(a)** Υ **(b)** m **(c)** H **(d)** Da on velocity with fixed values of ($F = 0.5, \epsilon = 0.1, \Upsilon = 0.1, x = 0.2, t = 0.2, l = 0.1$)

Figure 4 is plotted to highlight the influence of the Br, Sc, Sr, and H on the axial concentration. The reliance of concentration profile on Br and Sc are respectively described in Figures 4(a) and 4(b). The growing values of Brinkman number Br and Schmidt number Sc result in a decrease in concentration profile. Moreover, we look at Figures 4(c) and (d) to notice the influence of Soret number Sr and Hartman number H on the concentration profile. From these graphs, we observe that concentration diminishes with increasing Sr, but raises when we increase the effects of H.

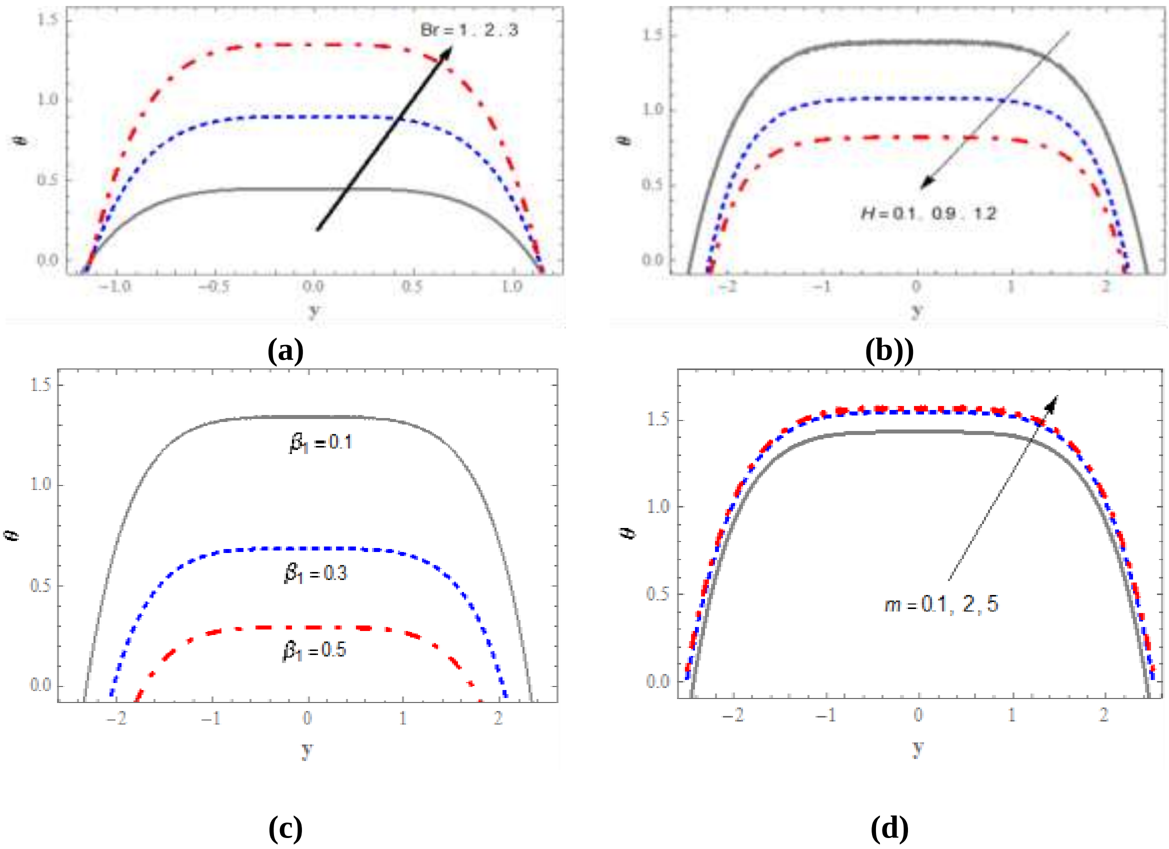

Figure 3: Influence of **(a)** Br **(b)** H **(c)** β_1 **(d)** m on temperature with fixed values of $(F = 0.5, \epsilon = 0.1, \Upsilon = 0.1, Da = 0.01, \beta = 0.5, m = 0.2, x = 0.2, t = 0.2, l = 0.1)$

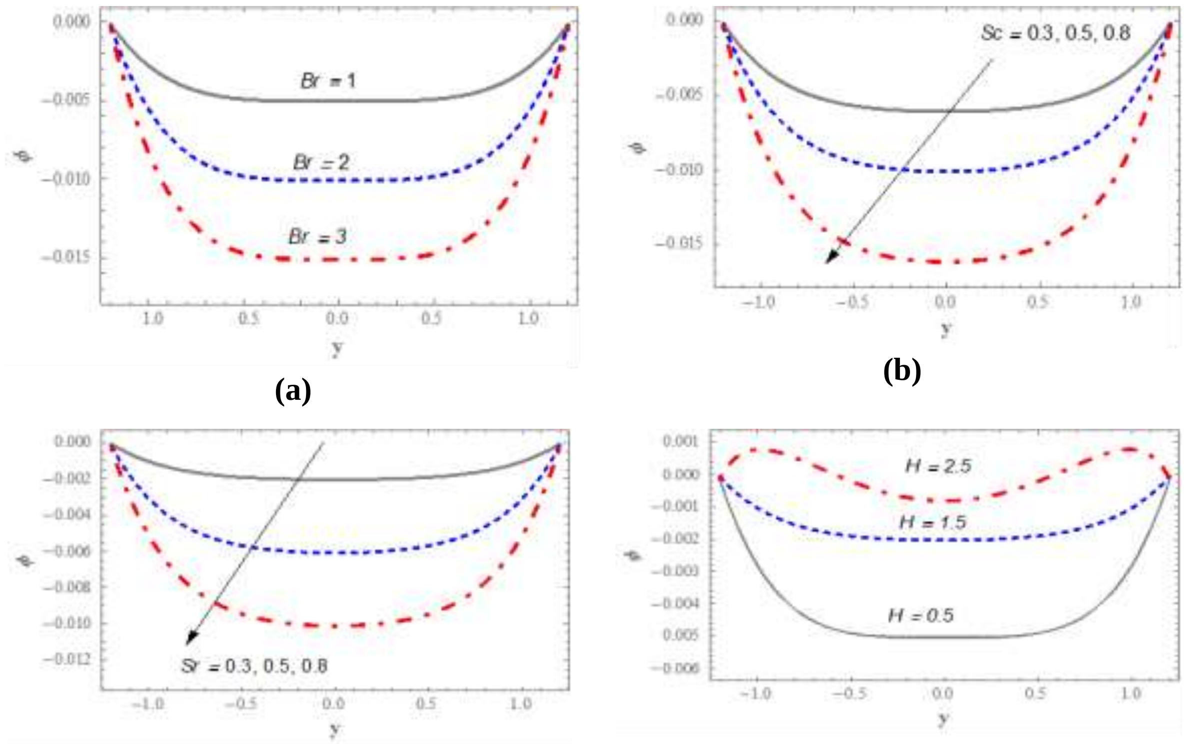

(a) (b)

(c) (d)

Figure 4: Influence of in (**a**) Br (**b**) Sc (**c**) Sr (**d**) H on concentration with fixed values of $(F = 0.5, \epsilon = 0.1, \Upsilon = 0.1, Da = 0.02, \beta = 0.5, m = 0.2, x = 0.2, t = 0.2, l = 0.1)$.

Trapping is an interesting phenomenon that denotes closed circulating streamlines that is at every elevated flow rate and when clogging up are very great. The influence of the velocity slip parameter β increases the trapped bolus size and number (Figure 5). It can be visualized from Figure 6 that when the coefficient of pseudo-plasticity Υ rises, the number of trapping decreases. Figure 7 shows that when the Hartman number H rises, the number and size of trapped bolus reduces. Because the Lorentz force opposes fluid flow and hence reduces fluid velocity, we note that bolus development can be avoided by adjusting the applied magnetic field's force. Further, Figure 8 depicts the impact of the Hall parameter m on the trapped bolus. A rise in m increases the size of the trapped bolus in this case.

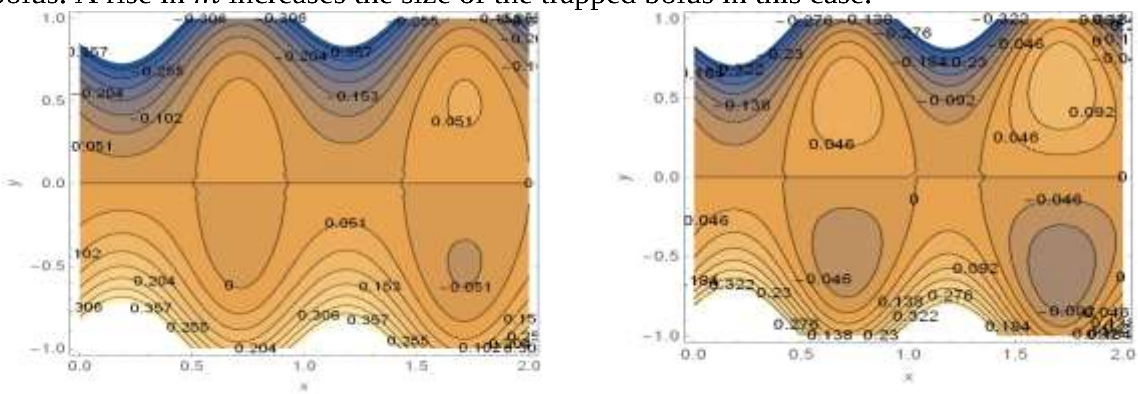

(a) (b)

Figure 5: Influence of (**a**) $\beta = 5$ (**b**) $\beta = 7$ on Stream function with fixed values of $(F = 0.5, \epsilon = 0.2, \Upsilon = 0.3, Da = 0.4, H = 0.1, m = 0.2, t = 0.7, l = 0.1)$

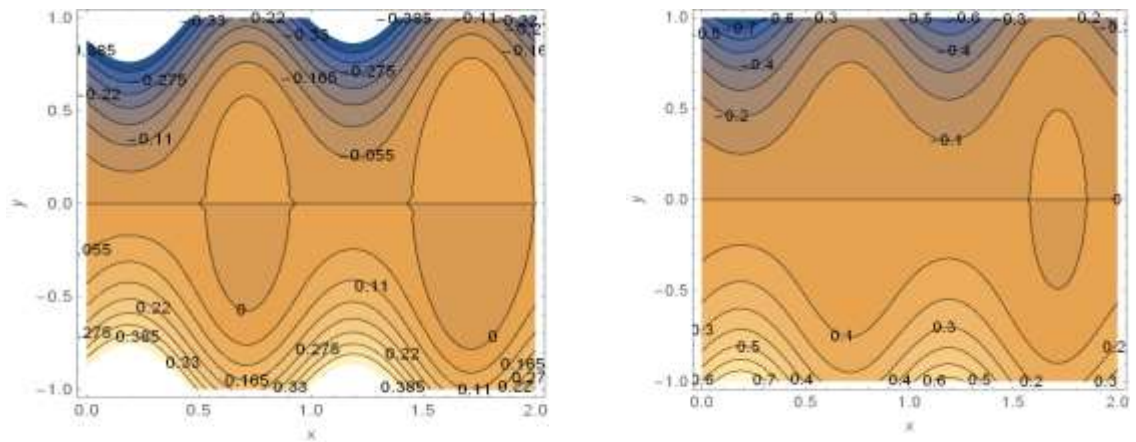

(a) **(b)**

Figure 6: Influence of (**a**) $\Upsilon = 0.3$ **(b)** $\Upsilon = 0.7$ on Stream function with fixed values of $(F = 0.5, \epsilon = 0.2, Da = 0.4, \beta = 4, H = 0.1, m = 0.2, t = 0.7, l = 0.1)$

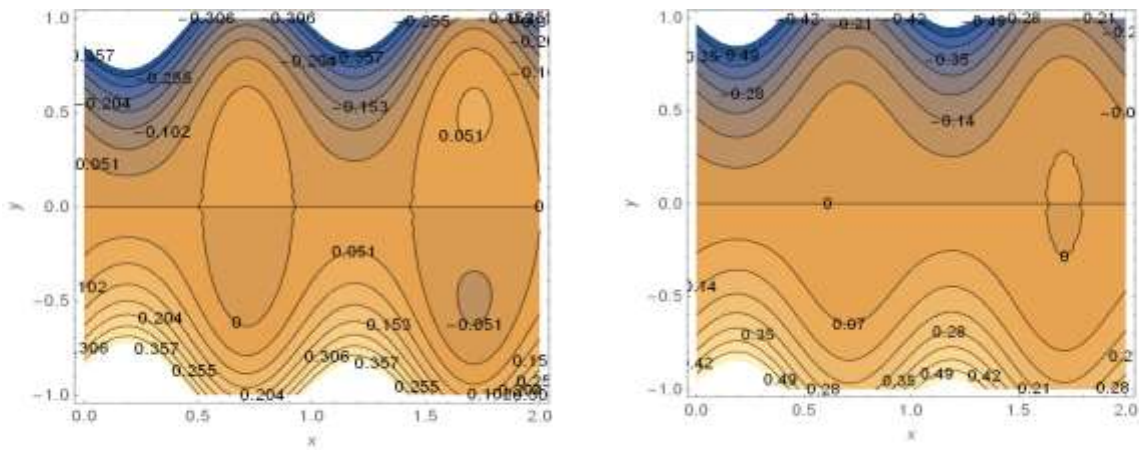

(a) **(b)**

Figure 7: Influence of (**a**) $H = 0.1$ **(b)** $H = 1$ on Stream function with fixed values of $(F = 0.5, \epsilon = 0.2, \Upsilon = 0.3, Da = 0.4, \beta = 5, m = 0.2, t = 0.7, l = 0.1)$

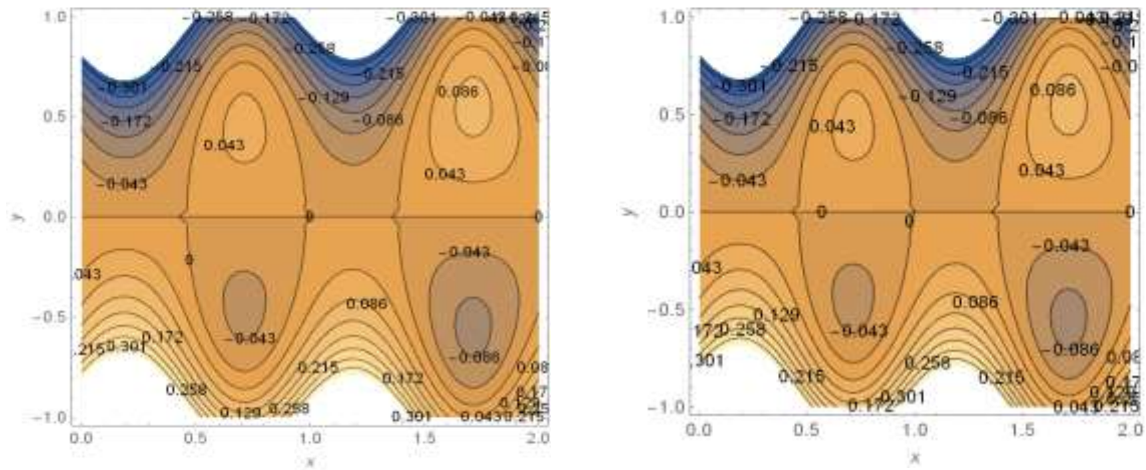

(a) **(b)**

Figure 8: Influence of (**a**) $m = 0.1$ **(b)** $m = 5$ on Stream function with fixed values of $(F = 0.5, \epsilon = 0.2, \Upsilon = 0.3, Da = 0.4, \beta = 6, H = 0.1, t = 0.7, l = 0.1)$

5. Conclusions

Influences of slip condition at the wall, the Hall current, and the Joule heating on the peristaltic influx through a tapered symmetric channel with permeable walls are studied analytically. From the aforementioned discussion, we deduce the following interesting observations:

- With an increase in the coefficient of pseudo-plasticity Υ, Hartman number H, and permeability parameter Da , there is a reduction in velocity u at the middle region of the channel. While a raise in Hall parameter m increases the velocity distribution.
- The absolute value of temperature improves with the growth of Brinkman number Br. Moreover, the temperature reductions with both of raising Hartman number H and thermal slip parameter β_1.
- An enhancement in Brinkman numbers Br, Sc, and Sr causes reduce in concentration profile. However, higher values of H show an increment in concentration distribution.
- By increasing the coefficient pseudo-plasticity Υ and Hartman number H, the number and size of trapped bolus are reduced. In addition, as the Hall parameter m and the velocity slip parameter β increase, the trapped bolus shifts to the right and grows in size.
- It is worth noting that our work is an extension of Hasen and Abdulhadi's [9] study, in which they investigated the effect of Soret and Dufour on Rabinowitsch Fluid flow, whereas we extended the research to investigate the effect of Heat and Mass as well as Hall and Joule Heating in a tapered Channel with Permeable Walls.

References

[1] A. I. M., S. A., M. El-Sayed, R.-G. Mohammad and H. Asiful, "Analysis of peristaltic flow of Jeffrey six constant nano fluid in a vertical non-uniform tube," *Chinese Journal of Physics,* vol. 66, pp. 60-73, 2020.

[2] A. A. Hayat, "Radiative peristaltic transport of Ree-Eyring fluid through porous medium in asymmetric channel subjected to combined effect of inclined MHD and convective conditions," *Journal of Physics: Conference Series,* no. 1879, 2021.

[3] M. M. and R. R. A., "Peristaltic transport of a Newtonian fluid in an asymmetric channel," *Z. angew. Math. Phys.*, vol. 54, p. 532–550, 2003.

[4] S. H. Saba and M. A. Ahmed, "Heat and mass impacts on peripheral layers of different viscosity on peristaltic flow of Rabinowitsch fluids," *AIP Conference Proceedings* , vol. 2292, no. 020007 , 2020.

[5] S. K. Rabiha and M. A. Ahmed, "Impacts of Heat and Mass Transfer on Magneto Hydrodynamic Peristaltic Flow Having Temperature-dependent Properties in an Inclined Channel Through Porous Media," vol. 61, no. 4, pp. 854-869, 2020.

[6] W. Sanae and H. Hirotsugu, "Hydrodynamic Lubrication of Journal Bearings by Pseudo-Plastic Lubricants," *Bulletin of JSM,* vol. 14, no. 69, pp. 268-278, 1971.

[7] N. M. Ehnber and N. Sohail, "Application of Rabinowitsch Fluid Model for the Mathematical Analysis of Peristaltic Flow in a Curved Channel," *Zeitschrift für Naturforschung A,* vol. 69, pp. 473-480, 2015.

[8] P. S. Udaya, G. R.S. and K. V.K., "On the Performance of Pivoted Curved Slider Bearings: Rabinowitsch Fluid Model," vol. 34, no. 3, pp. 128-137, 2012.

[9] S. H. Saba and M. A. Ahmed, "Analytical Study of Soret and Dufour effect in the Electro-osmotic peristaltic flow of Rabinowitsch fluid model," *Ibn AL-Haitham Journal For Pure and Applied Sciences,* vol. 34, no. 2, p. 70–86, 2021.

[10] V. Hanumesh, C. Rajashekhar, G. Manjunatha and V. P. Kerehalli, "Effect of variable liquid properties on peristaltic transport of Rabinowitsch liquid in convectively heated complaint porous channel," *Journal of Central South University* , vol. 26, p. 1116–1132, 2019.

[11] S. Hina and N. Sohail, "Analysis of Combined Convective and Viscous Dissipation Effects for," *Journal of Bionic Engineering,* vol. 14, no. 1, p. 182–190, 2017.

[12] R. M., E. R., M. S. Sadiq, M. M., S. S. M. and W. Ifraheem, "Enhancement of heat transfer in peristaltic flow in a permeable channel under induced magnetic field using different CNTs," *Journal of Thermal Analysis and Calorimetry* , vol. 140, p. 1277–1291, 2020.

[13] V. H, R. C, M. G, V. P. K, D. M. O and V. K, "Heat and mass transfer analysis of MHD peristaltic flow through a complaint porous channel with variable thermal conductivity," *IOP Publishing Physica Scripta,* vol. 95, no. 4, 2020.

[14] S. H. Saba and M. A. Ahmed, "MHD Effect on Peristaltic Transport for Rabinowitsch Fluid through A Porous Medium in Cilia Channel," *Iraqi Journal of Science,* vol. 61, no. 6, p. 1461–1472, 2020.

[15] S. K. Rabiha and A. M. Abdulhadi, "Effect of MHD and Porous Media on Nanofluid Flow with Heat Transfer: Numerical Treatment," *Journal of Advanced Research in Fluid Mechanics and Thermal Sciences,* vol. 63, no. 2, p. 317–328, 2019.

[16] A. A. Hayat and M. A. Ahmed, "Analysis of Heat Transfer on Peristaltic Transport of Powell-Eyring Fluid in an Inclined Tapered Symmetric Channel with Hall and Ohm's Heating Influences," *Journal of Al-Qadisiyah for Computer Science and Mathematics,* vol. 10, no. 2, pp. 26-41, 2018.

[17] H. T., A. Naseema, R. M. and E. Fuad, "Hall and Joule heating effects on peristaltic flow of Powell–Eyring liquid in an inclined symmetric channel," *Results in Physics,* vol. 7, pp. 518-528, 2017.

[18] H. Tasawar, Z. Hina, A. Ahmed and A. Bashir, "Hall current and Joule heating effects on peristaltic flow of viscous fluid in a rotating channel with convective boundary conditions," *Results in Physics,* vol. 7, pp. 2831-2836, 2017.

[19] R. Saravana, V. Kuppalapalle and S. S., "Influence of Compliant Walls and Heat Transfer on the Peristaltic Transport of a Rabinowitsch Fluid in an Inclined Channel," *Zeitschrift Naturforschung Teil A,* vol. 73, pp. 833-843, 2018.

[20] G. S. P., "On the Boundary Condition at the Surface of a Porous Medium," *Studies in Applied Mathematics,* vol. 50, no. 2, pp. 93-101, 1971.